Voronoi-Based Medial Axis Approximation from Samples: Issues and Solutions

Farid Karimipour and Mehran Ghandehari

Department of Surveying and Geomatics Engineering, College of Engineering, University of Tehran, Iran
{fkarimipr,ghandehary}@ut.ac.ir

Abstract. Continuous curves are approximated by sample points, which carry the shape information of the curve. If sampling is sufficiently dense, the sample points can be used to extract the structural properties of the curve (e.g., crust, medial axis, etc.). This article focuses on approximation of medial axis from sample points. Especially, we review the methods that approximate the medial axis using Voronoi diagram. Such methods are extremely sensitive to noise and boundary perturbations. Thus, a pre- or post-processing step is needed to filter irrelevant branches of the medial axis, which are introduced in this article. We, then, propose a new medial axis approximation algorithm that automatically avoids irrelevant branches through labeling sample points. The results indicate that our method is stable, easy to implement, robust and able to handle sharp corners, even in the presence of significant noise and perturbations.

Keywords: Sample points, Medial axis approximation, Pruning, Voronoi diagram, Delaunay triangulation.

1 Introduction

The Medial Axis (MA) was first introduced by Blum to describe biological shapes, and it is used as a tool in image analysis [1]. The MA is intuitively defined as follows: consider starting a fire at the same moment everywhere on the boundary of a shape in the plane. The fire propagates with homogeneous velocity in all directions. The MA is the set of points where the front of the fire collides with itself, or other fire front. Alternatively, in mathematical language, the MA is the set of points that are equidistant from at least two points on the boundary of the shape (Fig. 1).

The MA is used in a variety of applications including pattern analysis and shape recognition [2, 3], image compression [4], surface fitting [5], font design [6], path planning [7], solid modeling [8, 9], feature extraction in geometric design [10, 11] and Geospatial Information System (GIS) [12-14].

The methods proposed for the MA extraction are classified into discrete, semi-continuous and continuous (exact). In discrete case, the input and output are images. Different algorithms based on thinning [15], Voronoi diagram [16], distance transform [17] and mathematical morphology [18] are proposed in this class. In semi-continuous methods, the shape is approximated by a set of sample points on the shape

M.L. Gavrilova et al. (Eds.): Trans. on Comput. Sci. XX, LNCS 8110, pp. 138–157, 2013.

boundary and, then, the MA is extracted using these points based on different structures, say, Voronoi diagram of the sample points. The quality of the approximated MA directly depends on the sampling rate. Finally, in continuous algorithms the continuous shape is known and the exact MA is extracted. However, this is a complex problem and so far, the solution is known only for some geometrical shapes [19, 20].

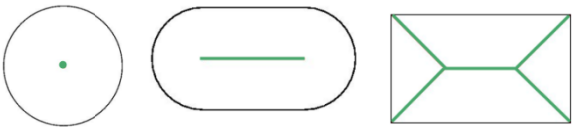

Fig. 1. The MA of some 2D shapes

A major issue of the MA is its inherent instability under small perturbations. The MA is very sensitive to small changes of the boundary, which produce many irrelevant branches in the MA corresponding to non-significant parts of the boundary, so as two very similar shapes can have significantly different MAs (Fig. 2). Filtering extraneous branches is a common solution to handle this issue. Some of the filtering methods work as a pre-processing step through simplifying (smoothing) the boundary before computation of the MA; The others prune the irrelevant branches of the extracted MA in a post-processing step.

The purpose of the filtering methods is to remove irrelevant branches, in order to preserve only the meaningful parts of the MA. In general, however, they may alter the topological or geometrical structure of the MA.

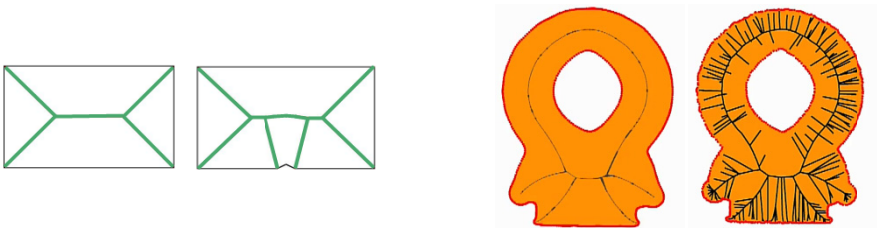

Fig. 2. Similar shapes may have significantly different MA due to boundary perturbations.

This article reviews the semi-continuous methods that use Voronoi diagram to approximate the MA from sample points. Furthermore, we introduce the most commonly used methods for filtering irrelevant branches of the MA, and discuss their main issues. This investigation has led us to proposing a new MA approximation algorithm that automatically avoids irrelevant branches through labeling the sample points. The results illustrate that our method is stable, easy to implement, robust and able to handle sharp corners, even in the presence of significant noise and perturbations.

The rest of the article is structured as follows: Section 2 presents some related geometric definitions, including the MA, sampling, Delaunay triangulation as well as Voronoi and power diagrams. In Section 3, the Voronoi-based algorithms proposed in

the literature for the MA approximation are reviewed. Some of the commonly used filtering methods are introduced in Section 4. In Section 5, we introduce our proposed algorithm for the MA approximation through labeling the sample points. Finally, Section 6 concludes the article and represents ideas for future work.

2 Geometric Preliminaries

This section represents some geometric definitions that are referred to in the following sections. It starts by a more detailed description of the MA. Two definitions related to sampling are then presented. Finally, Delaunay triangulation, Voronoi diagram and power diagram are introduced. In this section, $\mathcal{O}$ is a 2D object, $\partial\mathcal{O}$ is its boundary and $S \subset \partial\mathcal{O}$ is a dense sampling of $\partial\mathcal{O}$.

2.1 Medial Axis

Definition 1. The *medial axis* is (the closure of) the set of points in $\mathcal{O}$ that have at least two closest points on the object's boundary $\partial\mathcal{O}$ [21].

In 2D, the MA of a plane curve $\mathcal{O}$ is the locus of the centers of circles that are tangent to curve in two or more points, where all such circles are contained in $\mathcal{O}$ (Fig. 3.a). This article concentrates on the 2D MAs. However, this structure is also defined for objects of higher dimensions (Fig. 3.b).

(a) (b)

Fig. 3. The MA of (a) a curve in R^2 and (b) a surface in R^3

The *skeleton* is a concept closely related to the MA. Some literatures consider the skeleton equivalent to the MA [22], while some others believe they are similar, but are not equal [23]. In this article, we consider both the MA and the skeleton as equal terms and use the terms, interchangeably.

2.2 Local Feature Size and *r*-Sampling

Continuous curves are approximated by sampling. If sampling is sufficiently dense, the sample points carry the shape information of the curve, i.e., they can be used to reconstruct the original curve and approximate its MA. The quality of sample points S has a direct effect on curve reconstruction. *Local feature size* is a quantitative measure to determine the level of details at a point on a curve, and the sampling density needed for curve reconstruction.

Definition 2. The *local feature size* of a point $p \in \partial\mathcal{O}$, denoted as $LFS(p)$, is the distance from p to the nearest point m on the MA [21].

Note that $LFS(p)$ is different from radius of the medial circle, which is the tangent to curve at p (Fig. 4).

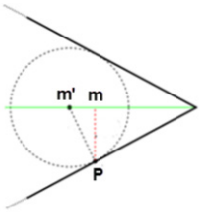

Fig. 4. The local feature size of a point p (pm) is not necessarily the same as the smallest radius of the medial circle touching p (pm') [24]

Definition 3. The object $\mathcal{O}$ is *r-sampled* by a set of sample points S if for each point $p \in \partial\mathcal{O}$, there is at least one sample point $s \in S$ that $\| p\text{-}s \| \leq r * LFS(p)$ [21].

The value of r is less than 1; and usually r=0.4 is considered a reasonably dense sampling [21]. Fig. 5 shows an example where sample points around the center are denser to provide a proper sampling.

(a) (b)

Fig. 5. (a) A curve with its MA; (b) An r-sampling of the curve [24]

The r-sampling factor is a lower bound for sampling that guarantees a proper reconstruction, but no upper bound was defined. Furthermore, such theoretical criteria may not be useful in practice. For instance, from a theoretical point of view, for sharp corners and noisy samples, infinite dense sampling is needed to guarantee the proper reconstruction, which is not practically possible [25, 26].

2.3 Delaunay Triangulation

Definition 4. Given a point set S in the plane, the *Delaunay triangulation* (DT) is a unique triangulation (if the points are in general position) of the points in S that satisfies the circum-circle property: the circum-circle of each triangle does not contain any other point $s \in S$ [27, 28]. Fig. 6.a illustrates a 2D example.

2.4 Voronoi Diagram

Definition 5. Let S be a set of points in R^2. The Voronoi cell of a point $p \in S$, denoted as $V_p(S)$, is the set of points $x \in R^2$ that are closer to p than to any other point in S:

$$V_p(S) = \left\{ x \in R^2 \,\middle|\, \|x - p\| \le \|x - q\|, q \in S, q \ne p \right\} \tag{1}$$

The union of the Voronoi cells of all points $s \in S$ forms the *Voronoi diagram* of S, denoted as $VD(S)$:

$$VD(S) = \bigcup V_p(S), p \in S \tag{2}$$

Fig. 6.b shows the Voronoi diagrams of a set of 2D points.

Delaunay triangulation and Voronoi diagram are dual structures: the centers of circum-circles of Delaunay triangulation are the Voronoi vertices; and joining the adjacent generator points in a Voronoi diagram yields their Delaunay triangulation (Fig. 6.c) [29].

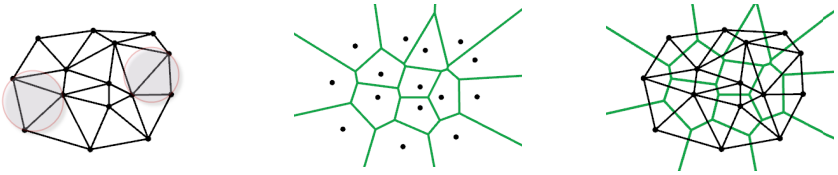

(a) (b) (c)

Fig. 6. (a) Delaunay triangulation and (b) Voronoi diagram of a set of points in the plane; and (c) their duality

For Voronoi diagram of sample points S, the Voronoi vertices are classified into *inner* and *outer vertices*, which lie inside and outside $\mathcal{O}$, respectively. Then, the Voronoi edges are classified into three groups: edges between two inner vertices (*inner Voronoi edges*), edges between two outer vertices (*outer Voronoi edges*), and edges between an inner and an outer vertices (*mixed Voronoi edges*).

A *Voronoi ball* is centered at a Voronoi vertex and its radius is its distance to the closest sample point. Again, Voronoi balls are classified into *inner* and *outer balls* depending on type of their center points [30].

2.5 Power Diagram

Power diagram is a weighted Voronoi diagram introduced by Edelsbrunner [31]. Suppose ball $B_{c,r}$ as a point c with weight r^2. The *power distance* between a point $x \in R^2$ and $B_{c,r}$ is:

$$d_{pow}(x, B_{c,r}) = \|x - c\|^2 - r^2 \tag{3}$$

Then:

Definition 6. Let S be a set of points in R^2. The *power diagram* is the subdivision of R^2 into cells and each cell of a point $p \in S$ is a set of points $x \in R^2$ that are closest, in power distance, to p (Fig. 7).

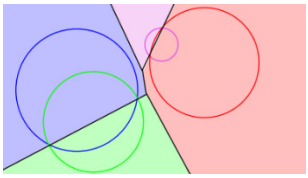

Fig. 7. The power diagram of four weighted points. A point c with weight r^2 is represented by a ball centered at c with radius r [32].

3 Voronoi-Based Algorithms for Medial Axis Approximation

This section introduces four Voronoi-based algorithms proposed in the literature to approximate the MA, including 'Voronoi ball', 'Voronoi edge', 'crust' and 'one-step crust and skeleton' algorithms.

3.1 Voronoi Ball Algorithm

This algorithm was proposed by Amenta *et al.* for the shape and MA approximation [32, 33]. Suppose $B = \{b_1, b_2, ..., b_n\}$ is the set of inner Voronoi balls and $U = \cup_{i=1}^{n} b_i$ is the union of these balls. The boundary ∂U of the shape U is composed of circular arcs, whose intersection points are referred to as $V(U)$. We also need to construct the dual of the union of the balls. For this, the power diagram of the points is computed (Fig. 8.a), and it is restricted to the union of the balls (Fig. 8.b). To compute the dual structure, for every edge in the restricted power diagram, an edge between the corresponding balls is added, and for every vertex in the corresponding restricted power diagram, a triangle constructed by the corresponding balls is created (Fig 8.c).

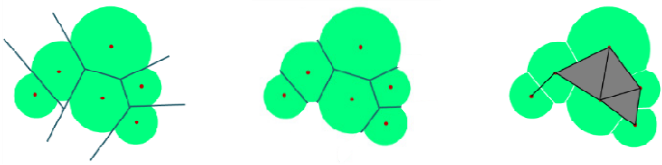

Fig. 8. Restricted power diagram and its dual: (a) Power diagram of the weighted points; (b) Power diagram restricted to the union of the balls; (c) Dual of the restricted power diagram

The Voronoi ball algorithm starts by constructing the Voronoi diagram of the sample points (Fig 9.b). Having computed the inner Voronoi balls (Fig 9.d), their union approximate the boundary of the shape (Fig 9.e). On the other hand, constructing the power diagram of the inner Voronoi vertices by assigning the radius of the balls as the weights results in the dual of the union of the balls (Fig 9.f). Finally, intersection of this dual structure with the Voronoi diagram of *V(U)* is an approximation of the MA of the shape (Fig 9.g and 9.h).

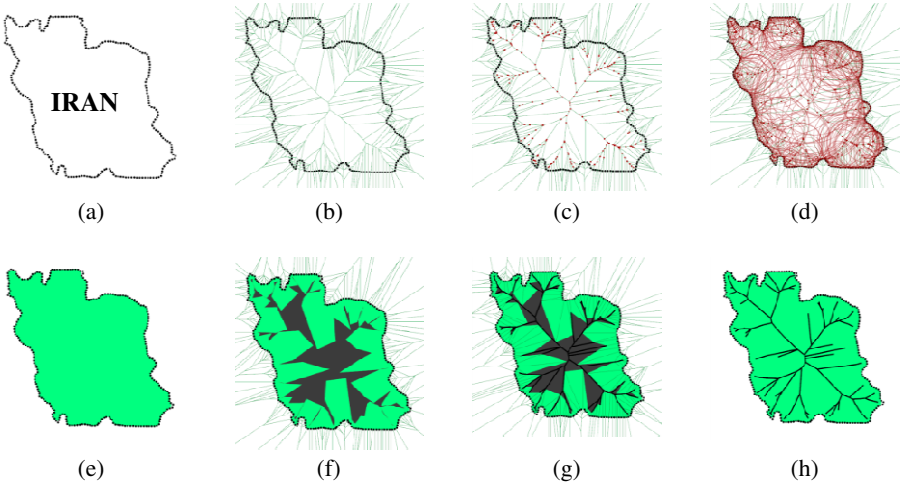

Fig. 9. The MA approximation using Voronoi balls method: (a) Sample points of the shape boundary; (b) Voronoi diagram of the sample points; (c) The inner Voronoi vertices; (d) The inner Voronoi balls, (e) Union of inner Voronoi balls, which approximates the shape, (f) Dual of the union of the balls; (g) Intersection of the dual and the Voronoi diagram of *V*(*U*); (h) Approximation of the MA of the shape.

This method is very computationally expensive. Furthermore, it is very sensitive to floating point arithmetic: A lot of Voronoi balls can intersect in one single point (Fig. 10.a) and a degenerate position in computation destroys the final results (Fig. 10.b).

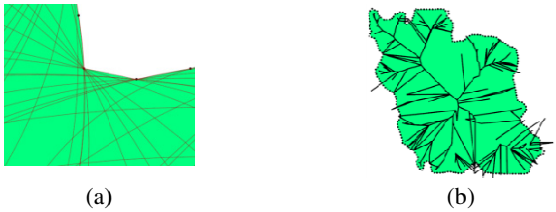

Fig. 10. Floating point arithmetic problems: (a) A lot of Voronoi balls can intersect in one single point and (b) degenerate position in computation destroy the MA.

3.2 Voronoi Edge Algorithm

Attali and Montanvert [34] has suggested that the union of the inner Voronoi edges can be interpreted as the MA (Fig. 11). It means that the MA edges are a subset of the Voronoi edges of the sample points (For more details and proofs, see [35]). The advantage of this algorithm is that it only needs computing a Voronoi diagram.

Fig. 11. The MA is a subset of the Voronoi edges

In another similar study, Tam [36] proposed the following steps for the MA approximation:

1. Compute the Delaunay triangulation of the sample points (Fig. 12.a).
2. Discard any triangles that are outside of the object (Fig. 12.b).
3. Compute the center of the circum-circles of remaining triangles (Fig. 12.c).
4. Construct the MA by connecting the centers of the circum-circles of the neighboring triangles (Fig. 12.d).

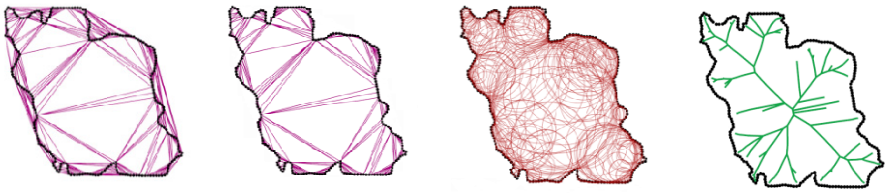

(a) (b) (c) (d)

Fig. 12. The MA approximation using Inner Voronoi edges: (a) DT of the sample points; (b) Discarding triangle that are outside the shape; (c) The circum-circles of remaining triangles; (d) Connecting the centers of the circum-circles of the neighboring triangles, which approximate the MA

3.3 Crust Algorithm

Amenta *et al.* [21] proposed a Voronoi-based algorithm (called crust algorithm) to reconstruct the boundary from a set of sample points forming the boundary of a shape. In this algorithm, the crust is a subset of the edges of the Delaunay triangulation of the sample points.

To compute the crust, let S be the sample points and V be the vertices of the Voronoi diagram of the sample points. Then:

1. Compute the Voronoi diagram of the sample points S (Fig. 13.a).
2. Compute the Delaunay triangulation of $S \cup V$ (Fig. 13.b).
3. The edges of the above Delaunay triangulation whose endpoints belong to S form the crust, which is an approximation of the shape (Fig. 13.b).

This algorithm can also be used for the MA approximation: the Voronoi edges extracted in step 1 whose dual Delaunay edges do not belong to the crust form the MA (Fig. 13.b).

The crust algorithm is based on the fact that an edge e of the DT belongs to the crust if e has a circum-circle that contains neither sample points nor Voronoi vertices of S. It means that a global test is needed to check the position of every sample points and Voronoi vertices respect to this circle.

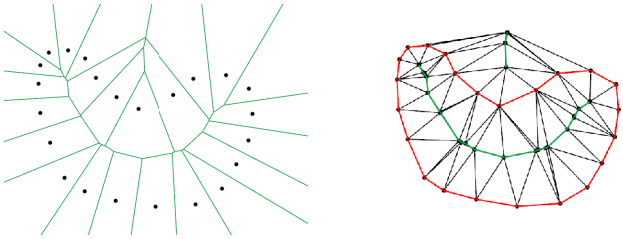

(a) (b)

Fig. 13. Curve reconstruction and the MA approximation using the crust algorithm: (a) Voronoi diagram of the sample points; (b) Delaunay triangulation of the sample points and Voronoi vertices

3.4 One-Step Crust and Skeleton Algorithm

Gold and Snoeyink [13] improved the crust algorithm so that both the boundary (crust) and the MA (skeleton) are extracted, simultaneously; and coined the name "one-step crust and skeleton" for this algorithm.

In the one-step crust and skeleton algorithm, every Voronoi/Delaunay edge is either part of the crust (Delaunay) or the skeleton (Voronoi), which can be determined by a simple *inCircle* test. Each Delaunay edge (D_1D_2 in Fig. 14.a) belongs to two triangles ($D_1D_2D_3$ and $D_1D_2D_4$ in Fig. 14.a). For each Delaunay edge, there is a dual Voronoi edge (V_1V_2 in Fig. 14.a).

Suppose two triangles $D_1D_2D_3$ and $D_1D_2D_4$ have a common edge D_1D_2 whose dual Voronoi edge is V_1V_2. The *InCircle*(D_1, D_2, V_1, V_2) determines the position of V_2 respect to the circle passes through D_1, D_2 and V_1. If V_2 is outside the circle, D_1D_2 belongs to the crust (Fig. 14.b). If V_2 is inside, however, V_1V_2 belongs to the skeleton (Fig. 14.c).

The value of $InCircle(D_1, D_2, V_1, V_2)$ test is calculated using the following determinant:

$$InCircle\ (D_1, D_2, V_1, V_2) = \begin{bmatrix} x_{D1} & y_{D1} & {x_{D1}}^2 + {y_{D1}}^2 & 1 \\ x_{D2} & y_{D2} & {x_{D2}}^2 + {y_{D2}}^2 & 1 \\ x_{V1} & y_{V1} & {x_{V1}}^2 + {y_{V1}}^2 & 1 \\ x_{V2} & y_{V2} & {x_{V2}}^2 + {y_{V2}}^2 & 1 \end{bmatrix} \tag{4}$$

D_1D_2 belongs to the crust if this determinant is negative, otherwise V_1V_2 belongs to the skeleton [13, 28, 37, 38].

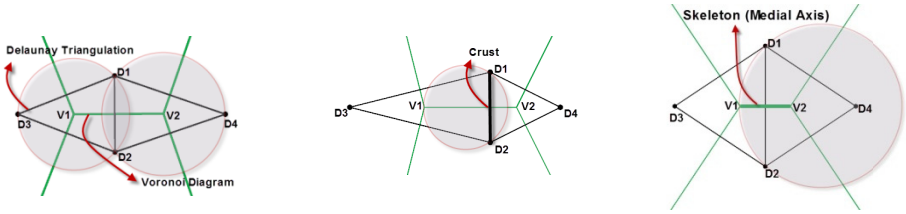

(a) (b) (c)

Fig. 14. One-step crust and skeleton extraction algorithm: (a) Delaunay triangulation and Voronoi diagram of four sample points D_1 to D_4; (b) V_2 is outside the circle passes through D_1, D_2 and V_1, so D_1D_2 belongs to the crust; (c) V_2 is inside the circle passes through D_1, D_2 and V_1, so V_1V_2 belongs to the skeleton.

The pseudo-code of the one-step crust and skeleton algorithm is as follows:

One-step crust and skeleton extraction
Input : Sample point S
Output: Crust and skeleton of the shape approximated by S

1. DT ← Delaunay Triangulation of S
2. E ← Edges of DT
3. For every $e \in$ E do
4. S_1, S_2 ← triangles that contain e
5. D_1, D_2 ← end points of e
6. V_1, V_2 ← centers of the circum-circles of S_1 and S_2
7. H ← $InCircle(D_1, D_2, V_1, V_2)$
8. If $H < 0$ then $D_1D_2 \in$ Crust
9. else $V_1V_2 \in$ Skeleton

As mentioned earlier, the global circle test used in the crust algorithm is replaced with a local test in the one-step crust and skeleton algorithm to assign the Delaunay/Voronoi edges to the crust and skeleton. Although it is simpler and faster, it may lead to assigning wrong edges to the crust. For example, in Fig. 15 the edge e is in the locally-defined crust because the circle passes through e does not contain the other Voronoi vertices of its dual Voronoi edge. However, e is not in the globally-defined crust because the circle passes through e includes some Voronoi vertices [13]. This problem is solved by satisfying the sampling conditions (see section 2.2).

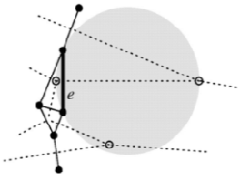

Fig. 15. The edge *e* (bold line) is in the locally-defined crust but it is not in the globally-defined crust [13]

4 Filtering the Extraneous Edges in the Medial Axis

As stated, the MA is sensitive to boundary perturbations. It results in many irrelevant branches in the MA corresponding to non-significant parts of the boundary, which must be filtered out. Such filtering may be applied as a pre-processing step through simplifying (smoothing) the boundary; or as a post-processing step through pruning, which eliminates the irrelevant branches of the extracted MA.

4.1 Simplification

Some of the filtering methods simplify the boundary before computing the MA by removing perturbations or boundary noises [39-42]. Although these methods aim to remove unwanted boundary noise, they may not provide the ideal results: the distinction between boundary data with noise could be difficult. In addition, these methods alter the topological structure and thus the MA position.

4.2 Pruning

The purpose of the pruning algorithms, as a post-processing step is to remove irrelevant branches in order to preserve only the stable parts of the MA. Different criteria were proposed in such algorithms to assign an *importance value* to each branch, and then the branches with the importance values less than a given threshold are removed [16, 43-48]. Typically, these criteria are based on angle, distance, area, etc.

Pruning algorithms have some drawbacks; (1) Some irrelevant branches may not be eliminated entirely. (2) Eliminating irrelevant branches usually shorten the main branches as well. (3) A disconnection in the main structure of the MA may be occurred. (4) Many of the pruning methods cannot preserve the topology of a complex shape. (5) In some cases, even multiple parameters are required and it is difficult to determine appropriate thresholds, simultaneously. Finally, most pruning methods do not work automatically and they require user checks at the end.

4.2.1 λ-medial Axis

Chazal and Lieutier [45] introduced the λ-medial axis pruning method. As Fig. 16 shows, they assign the importance values based on the distance between the contact

points (i.e., any Voronoi ball touches the boundary at contact points). They showed that the λ-medial axis preserves topology for a restricted range of values of λ and proved geometric stability with respect to small perturbations. However, λ is a global threshold and does not adopt the local size of the object.

Fig. 16. Importance values assigned by λ-medial axis method [49]

4.2.2 Angle Filtration

Attali and Montanvert [46] proposed an algorithm to prune the MA using an angular parameter. This angle is the maximum angle formed by the MA point, and its contact points (Fig. 17). They observed that the vertices of irrelevant branches have smaller bisector angles. No geometric stability guarantee has been presented for this method and its threshold depends on the distribution of sample points.

Fig. 17. Importance values assigned by angle filtration [49]

4.2.3 Discrete Skeleton Evolution

Bai and Latecki [47] introduced the discrete skeleton evolution as an area-based pruning method. The threshold in this method is the difference between the area of initial shape and the shape reconstructed from the simplified skeleton (Fig. 18). This method considers a weight w_i for each end branch, which is an edge of skeleton that has one junction point:

$$w_i = \frac{1 - A(R(S - P(L_i)))}{A(R(S))} \tag{5}$$

Where A is area function, S is the original skeleton, $P(L_i)$ is an end branch and $R(S)$ is the shape reconstructed from the skeleton.

(a) (b)

Fig. 18. Shape reconstruction from the MA: (a) Original shape and its MA; (b) The shape reconstructed from the MA [47]

Generally, an end branch with a small weight w_i has a little influence on the reconstruction, since the area of the reconstruction without this branch is nearly the same as the area of the reconstruction with it, so it can be removed [47]. Fig. 19 is the results of this algorithm for different thresholds.

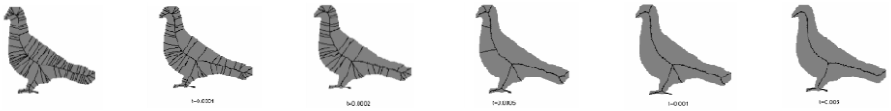

(a) (b) (c) (d) (e) (f)

Fig. 19. The skeleton evolution process results in iterative pruning of the skeleton of a bird: (a) The original skeleton; (b) to (f) The pruned skeletons with different thresholds [47]

This method shortens the main branches. Furthermore, finding an appropriate threshold is difficult.

4.2.4 Scale Axis Transform

In the λ-medial axis method, some main branches of the MA may be eliminated because the radius of their corresponding balls are smaller than the threshold. Replacing the global parameter for the whole shape with local parameters for each part of the shape is a solution to deal with this issue.

Giesen *et al.* [48] presented a different method called scale axis transform. They multiply the radius of all inner Voronoi balls by a certain simplification factor and consider their union as the grown shape. Then, the MA of the grown shape is considered as the simplified MA. Fig. 20 illustrates the steps of this method. The radius of the Voronoi balls is multiplied by a coefficient (multiplicative scaling) (Fig. 20.b). The Voronoi balls correspond to the less important branches are covered by larger balls (Fig. 20.c) and therefore small balls are eliminated. Thus, the MA of the grown shape keeps the whole main branches (Fig. 20.d). However, the result of this method may still contain some tiny extraneous branches (Fig. 21).

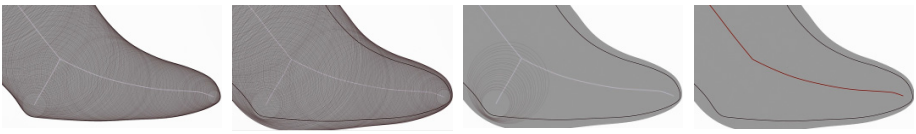

(a) (b) (c) (d)

Fig. 20. The steps of the scale axis transform algorithm: (a) The original MA and the inner Voronoi balls; (b) The radius of Voronoi balls is multiplied by a multiplicative scaling factor; (c) small balls are covered by larger balls; (d) The MA of the grown shape [48]

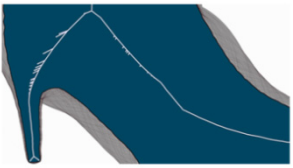

Fig. 21. Tiny extraneous branches in the MA after using the scale axis transform algorithm [48]

5 Proposed Approach for the Medial Axis Extraction

In this section we propose an improvement to the one-step crust and skeleton algorithm through labeling the sample points as a pre-processing; and show how our proposed approach improves the results [50].

Fig. 22.a illustrates the MA of a shape extracted using the one-step crust and skeleton algorithm. As this figure shows, this algorithm detects some extraneous edges as parts of the MA, which are filtered using simplification or pruning. However, we observed that such extraneous edges are the Voronoi edges created between the sample points that lie on the same segment of the curve. It led us to the idea of labeling the sample points in order to automatically avoid such edges in the MA (Fig 22.b).

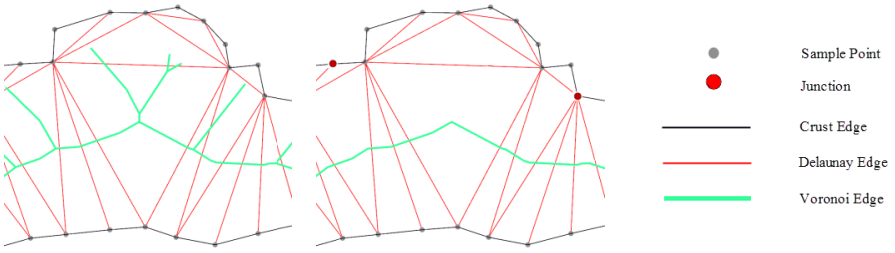

Fig. 22. (a) One-step crust and skeleton algorithm detects some extraneous edges as parts of the MA. They are the Voronoi edges created between the sample points that lie on the same segment of the curve; (b) our proposed method automatically avoid such edges in the MA.

We consider the shape boundary as different curve segments ∂O_i and:

$$\partial O = \bigcup_{i=1}^{n} \partial O_i \tag{6}$$

Inner and outer Voronoi edges do not intersect with ∂O, but mixed Voronoi edges do [30]. The same applied to the Delaunay edges: Delaunay edges of the sample points S are classified into three classes: *Mixed Delaunay edges* that join two consecutive points and belong to the crust; and *inner/outer Delaunay edges* that join two non-consecutive points and are completely inside/outside O (all Delaunay vertices lie on the ∂O). Note that the inner/outer/mixed Voronoi edges are dual to the inner/outer/mixed Delaunay edges.

We observed that the extraneous MA edges are the inner Voronoi edges (or its dual inner Delaunay edges) whose both end points lie on the same curve segment. However, the dual of the main MA edges are the inner Voronoi edges (or its dual inner Delaunay edges) whose end points lie on two different curve segment. Therefore, the main idea of the proposed approach is to remove all the MA edges whose corresponding Delaunay vertices lie on the same boundary curve.

We start with labeling the sample points: Each segment of the shape is assigned a unique label; and all of its sample points are assigned the same label. The points that are common between two curve segments are called *junctions*, which are assigned a unique negative label to distinguish them from other sample points.

Filtering in our proposed method is not a pre- or post-processing step, but it is performed simultaneously with the MA extraction. To extract the crust and MA, each Delaunay edge passes the *InCircle* test: If the determinant is negative and the corresponding Delaunay vertices have the same labels or one of them is a junction, that Delaunay edge is added to the crust. Otherwise, if the determinant is positive and the corresponding Delaunay vertices have different labels, its dual is added to the MA.

To apply our proposed approach in the one-step crust and skeleton algorithm, the lines 8 and 9 of the pseudo-code presented in section 3.4 are modified as follows:

---

8. If $H < 0$ and label(D_1)=label(D_2) or label(D_1)*label(D_2)<0 then $D_1D_2 \in$ Crust
9. else if label(D_1) ~= label(D_2) then $V_1V_2 \in$ Skeleton

---

Fig. 23 compares the result of one-step crust and skeleton algorithm and our proposed method. As it is illustrated, the resultant MA depends on the segmentation strategy: more junctions will result in a more complicated MA.

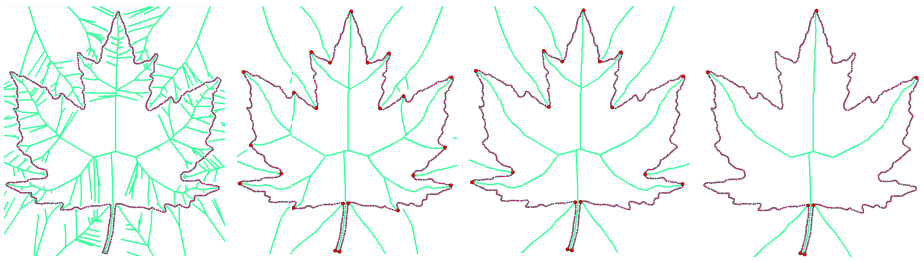

Fig. 23. The MA approximation: (a) One-step crust and skeleton algorithm; (b), (c) and (d) our proposed method for different segmentations: The more junctions, the more complicated MA

5.1 Stability

Stability is important because few sources of data are ideal. For stable algorithms, the MA should not be sensitive to the small changes of the boundary; in other words, small perturbations in the input data should not lead to large changes in the MA.

While existing methods apply a filtering process to remove the irrelevant branches, this issue is automatically solved in our labeling approach: The dual of proper edges in the MA are inner Delaunay edges whose end points lie on two different curve segments. Thus, if the end points of an inner Delaunay edge lie on the same curve segment, its dual inner Voronoi edge will be an irrelevant edge, which does not appear in the MA. Fig. 24 illustrates the results of one-step crust and skeleton algorithm and our approach for an example, before and after addition of boundary perturbations. As this figure shows, the perturbations do not have any effects on the final results.

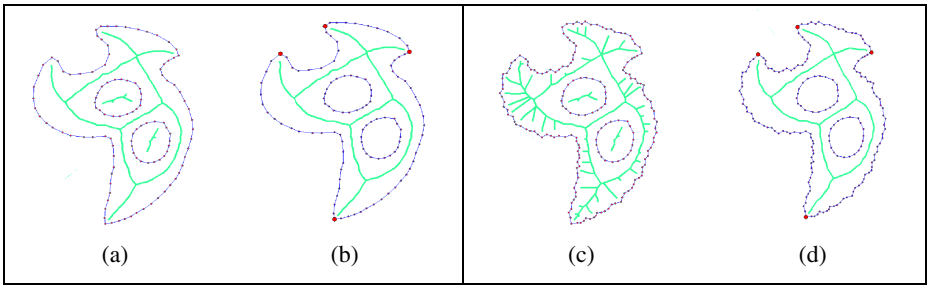

Fig. 24. The MA approximation before and after the addition of boundary perturbations: (a) and (c) One-step crust and skeleton algorithm; (b) and (d) our proposed method

5.2 Flexibility

Efficient algorithms for exact computation of the MA are only known for a few number of shapes [30]. Flexibility of proposed method increases the variety of shapes that can be used for the MA computation (Fig. 25). The shape and its complexity do not have any effect on the final results. This flexibility is due to labeling the sample points.

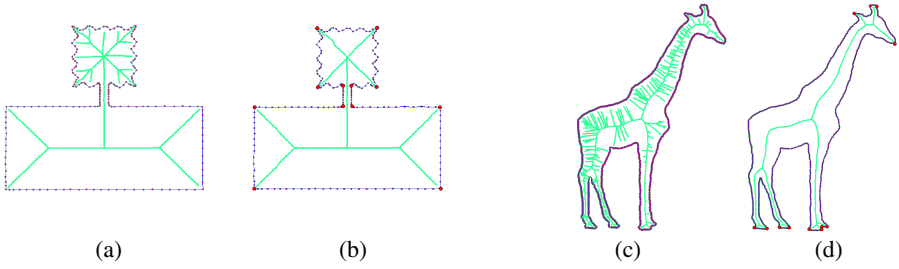

Fig. 25. The MA extraction: (a) and (c) One-step crust and skeleton algorithm; (b) and (d) our proposed method

5.3 Accuracy and Precision

The MA computation methods are classified into discrete, semi-continuous and continuous methods. The accuracy of semi-continuous methods depends on the density of

sample points: the more sample points, the more exact MA. The disadvantage of most existing methods is their low precision. Simplification and pruning which is done in most of the algorithms can alter the topological or geometrical structure of the MA. This problem is solved in the proposed method.

5.4 Complexity

Pruning algorithms are complex and repetitive, and does not work automatically, which results in high complexity and low speed of the MA extraction algorithm. Filtering in our method is not a pre- or post- processing step, but is integrated in the MA computation as a simple check and does not affect the running speed of the algorithm. Furthermore, complexity of all algorithms depends on the amount of noise and perturbation, while the complexity of our proposed method only depends on the number of sample points.

5.5 Handling Sharp Corners

Crust algorithm sometimes has problems in reconstructing curves at sharp corners, where the MA is very close to the boundary (Fig. 26). Based on sampling criteria, it requires infinite density sampling to guarantee the reconstruction process, which is not practically possible (high density of sample points leads to increasing the data volume and decreasing the speed of the algorithm). Another solution is arranging the sample points around all corners in an appropriate way, which is time-consuming for high volume data.

In our proposed approach, we detect the problematic shape corners through a post-processing step and only the sample points around these problematic corners needs rearrangement: After computing the crust, the number of crust lines joined at each junction is counted. If this number is less than a predefined threshold (usually 2 or 3), a rearrangement of sampling points is needed around this corner [51, 52].

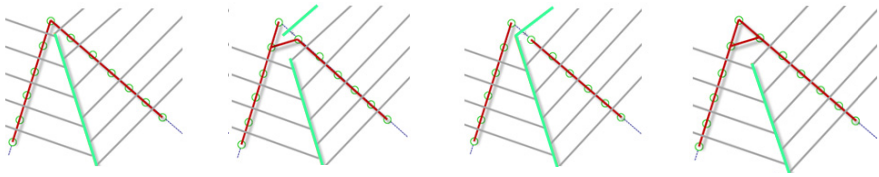

Fig. 26. Different states that may occur at sharp angles

6 Conclusion and Future Work

This article reviewed the MA approximation methods that use Voronoi diagram in their approach and improved one of the Voronoi-based MA extraction algorithms through labeling the sample points. It leads to a solution that is simple and easy to implement, robust to boundary perturbations, and able to handle sharp corners. The results show that

our proposed approach deals elegantly with different cases of sample points and solves the problems that may occur in other algorithms.

Simplification and pruning which is done in most of the algorithms can alter the topological or geometrical structure of the MA. The results illustrate that our method is stable, even in the presence of significant noise and perturbations, and have the same topology as the original MA.

In the future, we will extend the approach for surface reconstruction and 3D MA extraction. We will also study in more details the relationship between curve reconstruction and the MA extraction, as well as their applications in other fields.

References

1. Blum, H., et al.: A Transformation for Extracting New Descriptors of Shape. Models for the Perception of Speech and Visual Form 19, 362–380 (1967)
2. Blum, H., Nagel, R.N.: Shape Description Using Weighted Symmetric Axis Features. Pattern Recognition 10, 167–180 (1978)
3. Bookstein, F.L.: The Line-Skeleton. Computer Graphics and Image Processing 11, 123–137 (1979)
4. Brandt, J.W., Jain, A.K., Ralph Algazi, V.: Medial Axis Representation and Encoding of Scanned Documents. Journal of Visual Communication and Image Representation 2, 151–165 (1991)
5. Gross, L.M.: Transfinite Surface Interpolation over Voronoi Diagrams. PhD Thesis, Arizona State University (1995)
6. Chou, J.J.: Numerical Control Milling Machine Tool path Generation for Regions Bounded by Free Form Curves and Surfaces. PhD Thesis, University of Utah Salt Lake City, UT, USA (1989)
7. O'rourke, J.: Computational Geometry in C. Cambridge University (1998)
8. Gursoy, H.N., Patrikalakis, N.M.: Automatic Coarse and Fine Surface Mesh Generation Scheme Based on Medial Axis Transform: Part I Algorithms. Engineering with Computers (New York) 8, 121–137 (1992)
9. Sherbrooke, E.C., Patrikalakis, N.M., Brisson, E.: An Algorithm for the Medial Axis Transform of 3d Polyhedral Solids. IEEE Transactions on Visualization and Computer Graphics 2, 44–61 (1996)
10. Hisada, M., Belyaev, A.G., Kunii, T.L.: A Skeleton-Based Approach for Detection of Perceptually Salient Features on Polygonal Surfaces. Computer Graphics Forum 21, 689–700 (2002)
11. Hoffmann, C.M.: Geometric and Solid Modeling: An Introduction. Morgan Kaufmann (1989)
12. Gold, C.: Crust and Anti-Crust: A One-Step Boundary and Skeleton Extraction Algorithm. In: Proceedings of the Fifteenth Annual Symposium on Computational Geometry, pp. 189–196 (1999)
13. Gold, C., Snoeyink, J.: A One-Step Crust and Skeleton Extraction Algorithm. Algorithmica 30, 144–163 (2001)
14. Gold, C., Dakowicz, M.: The Crust and Skeleton–Applications in GIS. In: Proceedings of 2nd International Symposium on Voronoi Diagrams in Science and Engineering, pp. 33–42 (2005)

15. Lam, L., Lee, S.W., Suen, C.Y.: Thinning Methodologies-a Comprehensive Survey. IEEE Transactions on Pattern Analysis and Machine Intelligence, 869–885 (1992)
16. Ogniewicz, R.L., Kübler, O.: Hierarchic Voronoi Skeletons. Pattern Recognition 28, 343–359 (1995)
17. Borgefors, G.: Centres of Maximal Discs in the 5-7-11 Distance Transform. In: Proceedings of the Scandinavian Conference on Image Analysis, vol. 1, pp. 105–105 (1993)
18. Arcelli, C., Frucci, M.: Reversible Skeletonization by (5, 7, 11)-Erosion. In: Proceedings of the International Workshop on Visual Form: Analysis and Recognition, pp. 21–28 (1992)
19. Chou, J.J.: Voronoi Diagrams for Planar Shapes. IEEE Computer Graphics and Applications 15, 52–59 (1995)
20. Ramanathan, M., Gurumoorthy, B.: Constructing Medial Axis Transform of Planar Domains with Curved Boundaries. Computer-Aided Design 35, 619–632 (2003)
21. Amenta, N., Bern, M.W., Eppstein, D.: The Crust and the Beta-Skeleton: Combinatorial Curve Reconstruction. Graphical Models and Image Processing 60, 125–135 (1998)
22. Gonzalez, R.C., Woods, R.E.: Digital Image Processing. Prentice Hall, Upper Saddle River (2002)
23. Russ, J.C.: The Image Processing Handbook. CRC Press (2002)
24. Wenger, R.: Shape and Medial Axis Approximation from Samples. PhD Thesis. The Ohio State University (2003)
25. Cheng, S.W., Funke, S., Golin, M., Kumar, P., Poon, S.H., Ramos, E.: Curve Reconstruction from Noisy Samples. Computational Geometry 31, 63–100 (2005)
26. Dey, T.K., Wenger, R.: Fast Reconstruction of Curves with Sharp Corners. International Journal of Computational Geometry and Applications 12, 353–400 (2002)
27. Ledoux, H.: Modelling Three-Dimensional Fields in Geo-Science with the Voronoi Diagram and Its Dual. Ph.D Thesis. School of Computing, University of Glamorgan, Pontypridd, Wales, UK (2006)
28. Gavrilova, M., Ratschek, H., Rokne, J.G.: Exact Computation of Delaunay and Power Triangulations. Reliable Computing 6, 39–60 (2000)
29. Karimipour, F., Delavar, M.R., Frank, A.U.: A Simplex-Based Approach to Implement Dimension Independent Spatial Analyses. Journal of Computer and Geosciences 36, 1123–1134 (2010)
30. Giesen, J., Miklos, B., Pauly, M.: Medial Axis Approximation of Planar Shapes from Union of Balls: A Simpler and More Robust Algorithm. In: Canad. Conf. Comput. Geom., pp. 105–108 (2007)
31. Edelsbrunner, H.: The Union of Balls and Its Dual Shape. Discrete & Computational Geometry 13, 415–440 (1995)
32. Amenta, N., Choi, S., Kolluri, R.K.: The Power Crust. In: Proceedings of the Sixth ACM Symposium on Solid Modeling and Applications, pp. 249–266 (2001)
33. Amenta, N., Kolluri, R.K.: The Medial Axis of a Union of Balls. Computational Geometry 20, 25–37 (2001)
34. Attali, D., Montanvert, A.: Computing and Simplifying 2d and 3d Continuous Skeletons. Computer Vision and Image Understanding 67, 261–273 (1997)
35. Miklos, B., Giesen, J., Pauly, M.: Medial Axis Approximation from Inner Voronoi Balls: A Demo of the Mesecina Tool. In: Proceedings of the Twenty-third Annual Symposium on Computational Geometry, pp. 123–124 (2007)
36. Tam, R.C.: Voronoi Ball Models for Computational Shape Applications. PhD thesis, The University of British Columbia (2004)

37. Karimipour, F., Delavar, M.R., Frank, A.U.: A Mathematical Tool to Extend 2D Spatial Operations to Higher Dimensions. In: Gervasi, O., Murgante, B., Laganà, A., Taniar, D., Mun, Y., Gavrilova, M.L. (eds.) ICCSA 2008, Part I. LNCS, vol. 5072, pp. 153–164. Springer, Heidelberg (2008)
38. Alliez, P., Devillers, O., Snoeyink, J.: Removing Degeneracies by Perturbing the Problem or Perturbing the World. Reliable Computing 6, 61–79 (2000)
39. Mokhtarian, F., Mackworth, A.: A Theory of Multiscale, Curvature-Based Shape Representation for Planar Curves (Pdf). IEEE Transactions on Pattern Analysis and Machine Intelligence 14 (1992)
40. Siddiqi, K., Bouix, S., Tannenbaum, A., Zucker, S.W.: Hamilton-Jacobi Skeletons. International Journal of Computer Vision 48, 215–231 (2002)
41. Siddiqi, K., Kimia, B.B., Shu, C.W.: Geometric Shock-Capturing Eno Schemes for Subpixel Interpolation, Computation and Curve Evolution. Graphical Models and Image Processing 59, 278–301 (1997)
42. Attali, D., Montanvert, A.: Modeling Noise for a Better Simplification of Skeletons. In: Proceedings of the International Conference on Image Processing, vol. 3, pp. 13–16 (1996)
43. Attali, D., di Baja, G., Thiel, E.: Pruning Discrete and Semicontinuous Skeletons. In: Braccini, C., Vernazza, G., DeFloriani, L. (eds.) ICIAP 1995. LNCS, vol. 974, pp. 488–493. Springer, Heidelberg (1995)
44. Malandain, G., Fernández-Vidal, S.: Euclidean Skeletons. Image and Vision Computing 16, 317–327 (1998)
45. Chazal, F., Lieutier, A.: The "Lambda Medial Axis". Graphical Models 67, 304–331 (2005)
46. Attali, D., Montanvert, A.: Semicontinuous Skeletons of 2d and 3d Shapes. In: Aspects of Visual Form Processing, pp. 32–41 (1994)
47. Bai, X., Latecki, L.J.: Discrete skeleton evolution. In: Yuille, A.L., Zhu, S.-C., Cremers, D., Wang, Y. (eds.) EMMCVPR 2007. LNCS, vol. 4679, pp. 362–374. Springer, Heidelberg (2007)
48. Giesen, J., Miklos, B., Pauly, M., Wormser, C.: The Scale Axis Transform. In: Proceedings of the 25th Annual Symposium on Computational Geometry, pp. 106–115 (2009)
49. Mesecina: computational geometry you can see, http://www.balintmiklos.com/mesecina
50. Karimipour, F., Ghandehari, M.: A Stable Voronoi-Based Algorithm for Medial Axis Extraction through Labeling Sample Points. In: Proceedings of the 9th International Symposium on Voronoi Diagrams in Science and Engineering (ISVD 2012), New Jersey, USA, pp. 109–114 (2012)
51. Ghandehari, M., Karimipour, F.: Voronoi-Based Curve Reconstruction: Issues and Solutions. In: Murgante, B., Gervasi, O., Misra, S., Nedjah, N., Rocha, A.M.A.C., Taniar, D., Apduhan, B.O. (eds.) ICCSA 2012, Part II. LNCS, vol. 7334, pp. 194–207. Springer, Heidelberg (2012)
52. Karimipour, F., Ghandehari, M., Ledoux, H.: Medial Axis Approximation of River Network for Catchment Area Delineation. In: Proceedings of the International Workshop on Geoinformation Advances. Lecture Notes in Geoinformation and Cartography (LNG&C), p. 223. Springer, Johor (2012)